Journal of Cleaner Production 411 (2023) 137380

Contents lists available at ScienceDirect

Journal of Cleaner Production

journal homepage: www.elsevier.com/locate/jclepro

Characterization, LCA and FEA for an efficient ecodesign of novel stainless steel woven wire mesh reinforced recycled aluminum alloy matrix composite

Rubén Lostado-Lorza [a,*], Marina Corral-Bobadilla [a], Saúl Íñiguez-Macedo [b], Fátima Somovilla-Gómez [a]

[a] Department of Mechanical Engineering, University of La Rioja, C/ San José de Calasanz 31, 26004, Logroño, La Rioja, Spain
[b] Footwear Technology Center of La Rioja, C/ Raposal 65, 26580, Arnedo, La Rioja, Spain

ARTICLE INFO

Handling Editor: Cecilia Maria Villas Bôas de Almeida

Keywords:
Life cycle assessment
Finite element analysis
Metal matrix composite materials
Recycled materials
Mechanical properties

ABSTRACT

The production of metal matrix composites generally requires higher energy and raw materials consumption, while generating more waste than conventional material processing. The possibility of reusing recycled aluminum as an alternative in the production of metal matrix composites has led to the interest in this research as it can contribute to aluminum waste and raw reduction as well as to environmental impact mitigation. This paper provides an in-depth investigation of a brand-new metal matrix composite that is produced by gravity casting. In turn, the process is based on recycled aluminum EN AW 6082 for the matrix that is reinforced with stainless steel AISI 304 woven wire mesh that is intended for industrial and commercial use. A detailed description of the production procedure is reviewed, as are the vales of toughness, yield and tensile strengths that were determined by standardized tensile and Charpy tests. Life Cycle Assessment and Finite Element Analysis were used to determine, respectively, the environmental impact and the residual stresses generated during the production of the specimens for the above mentioned tests. Five different opening and wire diameter configurations for the AISI 304 woven wires were studied in this work. In a comparison to recycled aluminum alloy EN AW 6082 without reinforcement, the best results were provided by the 2.177 mm × 0.6 mm configuration. These results were the following: (1) Yield, tensile strength and toughness showed an increase of 245.5%, 13.62% and 175.0% respectively. (2) Life Cycle Assessment increased 8.31% for the highest environmental impact obtained (Human Toxicity). (3) The Finite Element Analysis showed that the residual stresses increased in their compressive values in −10.83 MPa, −9.925 MPa and −3.84 MPa, respectively, for the stainless steel wires, aluminum matrix and wire/matrix interfaces. From the mechanical properties, the environmental impacts and the residual stresses that were obtained, one can conclude that this study has demonstrated a technically feasible practical approach to the use of the recycled aluminum alloy EN AW 6082 using AISI 304 stainless steel woven wires as materials in the metal matrix composites production. This could lead to a substantial reduction in the volume of aluminum used and, consequently, provide environmental and economic benefits.

1. Introduction

The global market for metal matrix composites (MMC) is expected to grow by 6.4% between 2020 and 2027 due to the increasing use of lightweight materials with excellent technical properties in the automotive and aerospace industries. The increase in fuel prices and general the rise in the cost of energy has caused these materials to be used more and more in these industries (Newswire, 2020). However, MMC production usually requires greater consumption of energy and raw materials consumption while also generating more waste than does the production of conventional materials (Mussatto et al., 2021). MMC are base metals that have been reinforced with other materials (metals, organic compounds or ceramics). Titanium, magnesium or aluminum, along with their alloys, have attracted significant attention for use as the metal matrix in MMC, due to their low density and ease of production. Aluminum is the most widely used of these metals as its production cost

* Corresponding author.
E-mail addresses: ruben.lostado@unirioja.es (R. Lostado-Lorza), marina.corral@unirioja.es (M. Corral-Bobadilla), siniguez@ctcr.es (S. Íñiguez-Macedo), fatima.somovilla@unirioja.es (F. Somovilla-Gómez).

https://doi.org/10.1016/j.jclepro.2023.137380
Received 7 March 2023; Received in revised form 18 April 2023; Accepted 2 May 2023
Available online 3 May 2023

is relatively low (Sharma et al., 2020). However, the production of aluminum is responsible for around 1% of the world's greenhouse gas emission. In addition, according to the International Aluminium Institute (2009), it is estimated that in 2019 approximately 32 million tons of aluminum waste was not recycled and, instead, ended up in landfills or was otherwise treated. This amount of unrecycled aluminum has aroused the interest of the authors of this study. Thus, the possibility of reusing recycled aluminum as an option in the production of MMC is raised with the ultimate purpose of reducing aluminum waste generation, raw and energy consumption, as well as mitigating environmental effects. Furthermore, the materials that are most often used as reinforcement in MMCs are carbon and metallic fibers, aluminum oxide, boron carbide and silicon carbide. They are usually integrated into the matrix as particles or fibers. These reinforcing materials are what give MMCs an increase in their strength, resistance to corrosion, thermal conductivity, fatigue life and wear resistance. The metallic fibers of stainless steel, nickel and titanium are the most commonly used metallic fibers in MMC. However, stainless steel fibers the least studied, despite being the most economical fibers and widely used both in industry and in domestic applications. It is also easy to work and process (Mortensen and Llorca., 2010). Although aluminum and stainless steel are two attractive materials for the production of MMCs', few researchers have recently studied in depth the mechanical properties of MMCs' aluminum matrix reinforced with stainless steel fibers or woven wires (Pinnel and Lawley., 1970; Pattnaik et al., 1974; Bhagat, 1988). These studies demonstrated that, regardless of the manufacturing process, an evident substantial improvement in the mechanical properties of the aluminum matrix is achieved when the latter is reinforced with stainless steel wires. However, to date no further in-depth studies have been found in which recycled aluminum has been used as a matrix or in which stainless steel woven wire mesh that is intended for industrial and commercial use has been employed as a reinforcement material in the production of MMC. Although MMCs have strong mechanical characteristics, thermal residual stresses have a substantial negative impact on their mechanical properties and behavior. As a consequence, thermal residual stress prediction and measurement are critical to ensure that a MMC presents a stress state of its reinforcing material, matrix and reinforcement/matrix interfaces below the yield strength of both materials. Therefore, it is desirable that both the reinforcing material and the reinforcement/matrix interfaces of any MMC have compressive thermal residual stresses as low as possible (Aghdam and Morsali., 2014). Finite Element Analysis (FEA) is a numerical method that makes possible to determine theoretically and accurately the thermal residual stresses that occur during the cooling process of MMCs. However, no in-deep studied have been found in which thermal residual stresses have been determined for aluminum matrix that are reinforced with stainless steel fibers or woven. Some researchers have determined the thermal residual stresses with the FEA when the reinforcing material was inserted into the matrix in particle form (Ahmad et al., 2020, González et al., 2023). In both studies, the results showed that the residual stresses in both the reinforcement material and the reinforcement/matrix interfaces reached compression values, thus confirming that the proposed MMc cooling process was appropriate (Aghdam and Morsali., 2014). Although MMC has good mechanical properties, it is well known that producing them requires considerable consumption of energy and raw materials, as it is necessary to fuse the matrix material. Therefore, Life Cycle Assessment (LCA) is often used to determine how much energy and raw materials were used and, also, the extent to which emissions and waste from a process or product affect the environment. A few researchers have undertaken on LCA on MMC to investigate the environmental effect for producing this type of materials. Most of the research has focused on synthetic fibers (carbon glass or aramid) (Umair, 2006), polymer composites reinforced with natural fibers (Fitzgerald et al., 2021; Wu et al., 2018). Very few were intensive studies of metal matrix composites (Yusuf et al., 2021, Santiago et al., 2022). The authors of all of the cited studies concentrated on the LCA of the MMC manufacturing process, but did not analyzed the mechanical properties of the MMC. However, more recently, Eguía et al. (2022) developed a preliminary study of some configurations of AISI 304 stainless steel bidirectional continuous fibers inserted in recycled aluminum EN AW-6082 to determine the environmental impact of producing the proposed MMC as well as the yield, tensile strength and toughness. Given the challenges that increased consumption of energy and raw materials generate worldwide due to population growth, urbanization and economic development, which have led to increased pressure on natural resources and growing concern for sustainability and climate change, this research explores the feasibility of producing a brand-new MMC. Because it is possible to employ recycled and commonly used materials, which would have positive environmental, economic and social consequences, the new MMC that this paper proposes provides the following novelties with respect to other commonly used and already studied MMC: (1) the material matrix is recycled aluminum EN AW 6082, (2) the reinforcing material is stainless steel AISI 304 woven wire mesh that is intended for industrial and commercial use and (3) the brand-new MMC is manufactured by gravity casting. Five different openings and wire diameters configurations oriented at 0° of AISI 304 woven wire mesh that is intended for industrial and commercial use were studied to determine which has the best mechanical properties while minimizing its thermal residual stresses and its environmental impact produced during the manufacturing process. They were: (opening x wire diameter) 1.41 mm × 0.32 mm; 1.81 mm × 0.5 mm; 2.177 mm × 0.6 mm; 2.72 mm × 0.75 mm and 2.828 mm × 0.8 mm. Mechanical properties such as toughness, yield and tensile strength were determined by standardized tensile and charpy tests. The manufacturing process of those specimens that were used in the tensile and charpy tests served as a starting point in the determination of the thermal residual stresses and the environmental impacts. The latter were determined by a 3D elastoplastic thermo-mechanical FEA and the LCA, respectively. The results contrasted with those of the recycled aluminum EN AW 6082 without reinforcement. Finally, faults and imperfections, the wettability of the interaction between aluminum and stainless steel and the significant elements of the proposed MMC were determined by X-ray radiography analysis, Scanning Electron Microscopy (SEM) and Energy Dispersive X-ray (EDX), respectively. Fig. 1 summarizes the methodological workflow that was followed in this study of the feasibility of producing the proposed brand-new MMC and also determining the best configuration of opening x wire diameter of the considered AISI 304 woven wire mesh that is intended for industrial and commercial use.

2. Materials and methods

2.1. Casting process of recycled aluminum

The procedure to produce MMCs must establish a strong connection between matrix and reinforcement while avoiding interfacial reactions. There are a few different ways to produce MMCs, all of which have been used effectively for decades. They include infiltration with casting, liquid metal and deposition techniques like plasma spraying. Gravity, compocasting, squeeze casting or low-pressure casting can be used to manufacture the MMC. Gravity casting the is most economical process as it requires the least energy (Board, 1988). All of the MMCs that were studied in this work were produced by a gravity casting technique. The following procedures were closely adhered to in the production of all wire configurations that were studied. This was ensured that there was optimal matrix-to-reinforcement bonding and interfacial reactions were avoided. Thus, an AISI 310S stainless steel rectangular mold was used as a crucible, and the recycled aluminum alloy EN AW 6082 was melted in it, and formed part of the metal matrix. The AISI 310S stainless steel crucible had a capacity of 190 mm × 70 mm x 60 mm (Fig. 2a). A Hobersal muffle furnace type HK-11 (Hobersal, Spain), which can operate at a maximum temperature of 1000 °C, was employed to melt the recycled aluminum. Then, after the furnace had reached a consistent

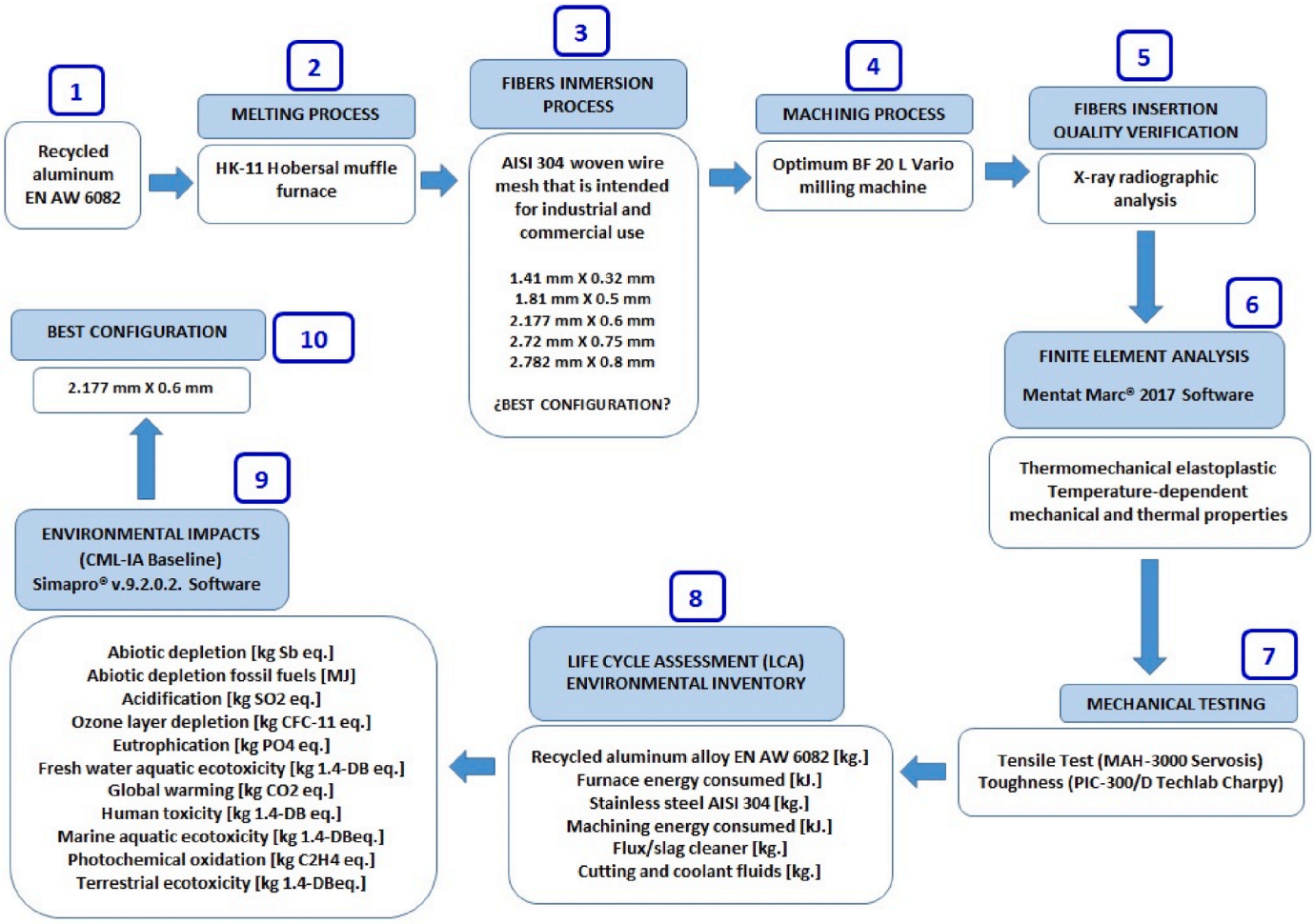

Fig. 1. Methodological workflow.

temperature of 800 °C, the solid recycled aluminum and the mold were placed inside where they remained for 2 h. When the temperature of the aluminum in the furnace had reached the melting point (660 °C), the flux/slag cleanser FLUX 50 was added. The quantity of flux/slag cleaner that was used was equal to 0.5% of the weight of the recycled aluminum (approximately 8 g). This flux/slag cleanser was added to the aluminum casting process to eliminate all waste products and impurities. It also prevented the oxidation of the molten aluminum when the latter was exposed to air in the HK-11 Hobersal muffle furnace. After the recycled aluminum had been molten for 2 h, the stainless steel crucible that contained the liquid aluminum was extracted from the muffle furnace and brought to room temperature on a refractory surface. (Fig. 2b). The layer of slag that had accumulated on the aluminum's surface was removed. It consisted of a mixture of fluxes, aluminum oxides and slag. Then, to form symmetric specimens of stainless steel/recycled aluminum MMCs, the stainless steel AISI 304 woven wire mesh that is intended for industrial and commercial use was inserted vertically into the middle of the crucible and the liquid aluminum by means of a tool that was made of stainless steel AISI 304. This tool was used to fully immerse the 304 stainless steel mesh vertically into the molten recycled aluminum. This served to reduce the deformation of the stainless steel woven wires while the aluminum cooled. The tool consisted of a square-sectioned top guide and a round-sectioned bottom guide. This tool used to keep the stainless steel AISI 304 woven wires straight. It is shown in Fig. 2c. In this example, the guide has a wire opening of 2.828 mm and a wire diameter of 0.8 mm. Fig. 2d depicts the assembly of the tool, the crucible and 304 stainless steel grid after exposure to the recycled aluminum alloy EN AW 6082 liquid at a temperature of 800 °C. Then, the crucible, the assembly tool, and the stainless steel AISI 304 woven wires were immediately reintroduced to the muffle furnace at a temperature of 800 °C, while the furnace was disconnected. This last procedure served to regulate the rate of cooling for each of the investigated MMC's configurations. It takes about 20 h to lower the temperature inside the muffle furnace from 800 °C to 20 °C.

2.2. Machining process of stainless steel/recycled aluminum MMC wire configurations

After approximately 20 h, when the interior temperature of the muffle furnace had already reached 20 °C, the aluminum block that housed the stainless steel woven wires was removed from the stainless steel crucible. The dimensions of each of these aluminum blocks were 190 mm × 70 mm x 50 mm. These were sufficient to obtain the specimens that corresponded to the ISO 6892 (2019) and ISO 14556 (2015) tensile and charpy tests respectively for all configurations that were studied. All specimens were machined with an Optimum milling machine (Optimum, Germany), using a face mill cutter that enabled machining by face milling. The powers consumed when milling the specimens for the tensile and charpy tests was determined according to Equation (1) (Walsh, 2001). For all configurations that were studied, the metal removal rate *(MRR)* and the specific energy for machining the material (*w*) were calculated according to:

$$Milling\ power\ [J/s] = MRR \bullet \omega \quad (1)$$

For the recycled aluminum, a value of 0.75 GJ/m^3 was assumed *w* in this

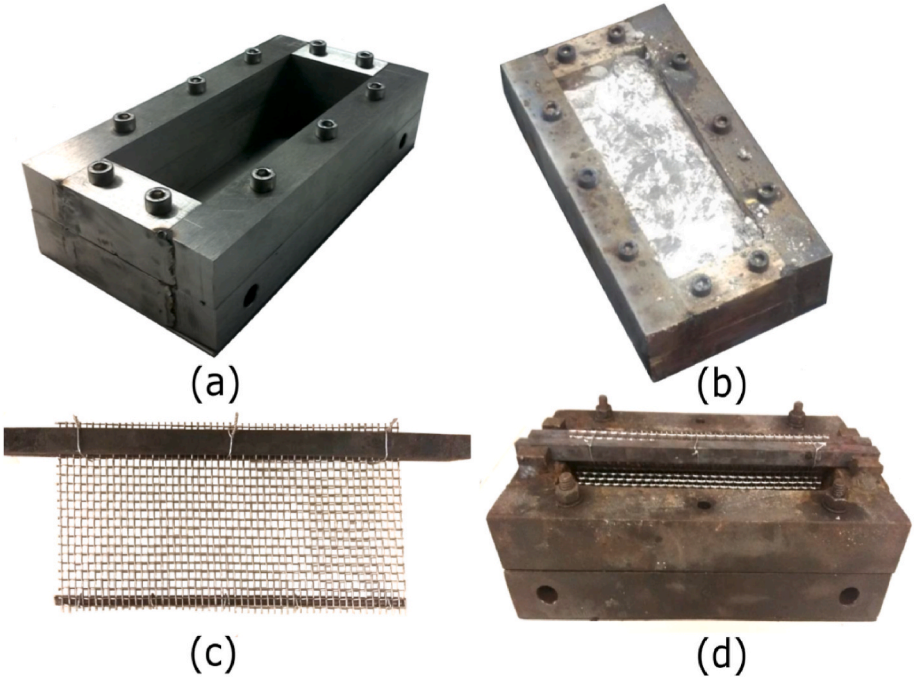

Fig. 2. (a) Stainless steel AISI 310S crucible. (b) Molten aluminum with the slag layer deposited on the surface. (c) The tooling designed to introduce the perfectly flat and straight stainless steel woven wires into the cast aluminum. (d) The stainless steel woven wires in the molten aluminum are ready for reintroduction to the muffle furnace, the temperature of which is approximately 800 °C.

case. In addition, when a face mill cutter is used with a milling machine, the value of MRR can be determined according to Equation (2):

$$MRR\ \left[mm^3\ /\ min\right] = Chip\ area \bullet V_f \bullet K = A_p \bullet A_e \bullet V_f \bullet K \tag{2}$$

MRR is determined from the axial (A_p) and radial depths of cut (A_e), as well as the cutting speed (V_f) and the unit constant (K). Since the material to be machined was recycled aluminum alloy EN AW 6082 and the performance of the Optimum milling machine was well known, the parameters that were assumed were $A_p = 3$ mm, $A_e = 50$ mm, $V_f = 100$ mm/min and K = 0.001. Finally, the net energy consumed in the machining process can be determined by Equation (3) which considers the total volume of aluminum to machine (V_{al}) for each of the specimens, the performance of the milling machine (η) and the MRR obtained (Diaz et al., 2011). In this case, the performance (η) for the Optimum milling machine was assumed to be 0.85.

$$Net\ energy\ [J] = \frac{V_{al}}{MMR \bullet \eta} \bullet Milling\ power \tag{3}$$

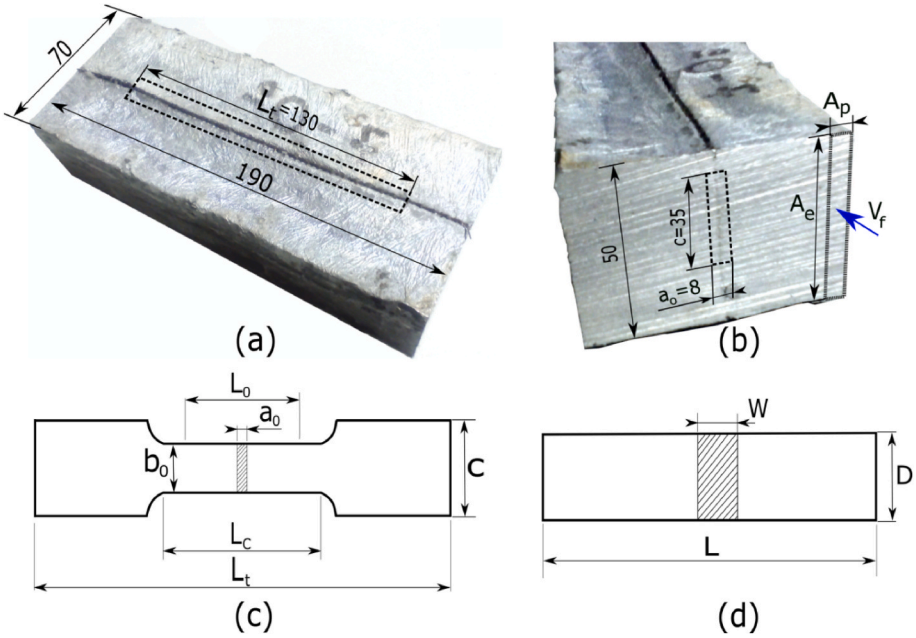

Fig. 3. (a) Details of the demolded block of recycled aluminum alloy EN AW 6082 ready for milling and displaying the completely integrated stainless steel AISI 304 woven wire mesh. (b) Details of the aluminum block's cross-section and specimen's general dimensions for the tensile test. (b) Dimensions of the specimen for the tensile test, as specified in Annex D of ISO 6892. (c) Toughness specimen dimensions according to the Charpy flatwise impact specimen without a notch.

Machining of the specimens uses cutting and coolant fluids in an effort to reduce the energy consumed by the each step and to improve the surface finish. They are necessary to provide proper cooling and lubrication in all cutting operations (Sarikaya et al., 2021). The rate of tool failure is hastened by the tool-to-workpiece friction. The latter causes extremely high wear rates and high cutting temperatures (Öndin et al., 2020). In many machining processes, the use of cutting fluids has become essential in order to reduce both, forces and temperatures that appear when cutting materials (de Martini Fernandes et al., 2019). In this case and because $V_f = 100$ mm/min, a cutting and coolant fluid loss due to evaporation of 0.4 kg/min was estimated by Iqbal et al. (2021). Fig. 3 depicts the aluminum block that was removed from the crucible. The remains of the inserted stainless steel grid are visible on its surface. This figure also shows the dimensions of the specimens that were used for the tensile and charpy tests. Fig. 3a and b shows that the stainless steel woven wires are positioned precisely in the middle of the aluminum block. These figures show, in dashed lines, the contour of the specimen that can be obtained by milling machine for the tensile test (L_t = 130 mm x C = 35 mm). A cross-sectional view of the aluminum block in Fig. 3b reveals a perfectly vertical stainless steel woven wire mesh that is completely implanted in the aluminum matrix. Fig. 3b also shows the direction of the machining in which A_p; A_e and V_f can be seen. Fig. 3c indicates the dimensions of the specimens that are used in the tensile tests, as specified by Annex D of ISO 6892 ″Non-proportional test pieces." They are $a_0 = 8$ mm, $b_0 = 28$ mm, $c = 35$ mm, $L_0 = 85$ mm, L_c = 100 mm and L_t = 130 mm. Standardized Charpy impact specimens without notches, and measuring 55 mm in length (L), 10 mm in width (D), and 8 mm in thickness (W), were used to measure toughness. They can be seen in Fig. 3d. This method of manufacturing the recycled aluminum alloy EN AW 6082 that is reinforced with stainless steel AISI 304 woven wire mesh was used to manufacture all specimens for the study of the five wire configurations and, also, the recycled aluminum alloy without reinforcement.

2.3. Finite Element analisys

Residual stresses are those that remain in a body despite the absence of an applied force. The assessment of the distribution and magnitude of these stresses in MNC is essential because they influence their mechanical and physical properties (Requena et al., 2012). They are usually generated in MMC by the manufacturing process (milling, tuning, drilling, etc.) or by temperature changes and gradients (casting or thermal treatments). Thermal residual stresses are sometimes enough to trigger plastic deformation of the matrix near the fiber. They are generated by the disparity between the matrix and fiber coefficients of thermal expansion in the MMC after the material has cooled to room temperature. Significant residual tensile stresses in the matrix hasten the yielding of the structure, whereas residual compressive stresses at both the fiber/matrix interface and the fibers delay the onset of damage to the interface under transverse loading (Aghdam and Morsali., 2014). It is a common practice to define "initial yield" as the stress at which the matrix's most severely loaded point yields and collapses due to the MMC's inability to withstand further loading. For a structural analysis of MMC components, the initial yield strength is overly conservative, especially if the residual stresses are considered. One of the strengths of FEA is the possibility that this numerical method offers for obtaining precise distributions of residual stress and strain in the matrix, fiber/-matrix interfaces and fiber in MMC. These are necessary for a good understanding of the mechanical behavior of composites (Li and Wisnom., 1994). In the current paper, a three-dimensional thermo-mechanical elastoplastic FEA using Mentat-Marc software (2014) was employed in this work to determine, for each opening and wire diameter configuration that was studied, the thermal residual stresses in the local X direction of the unit cell (RS_X) and those in the local Y direction of the unit cell (RS_Y). This was done for the stainless steel AISI 304 woven wire mesh, for the recycled aluminum alloy EN AW 6082 matrix and for the wires/matrix interfaces. It can be assumed because recycled aluminum EN AW 6082 without reinforcement lacks stainless steel wires inside. This, it is assumed, is why the cooling rate is very low and why the residual stresses on this material without reinforcement could be considered as depreciable. Therefore, in this work, we did not determine the residual stresses of the recycled aluminum EN AW 6082 without reinforcement by using FEA. They were determined only for the configurations proposed with stainless steel AISI 304 woven wire mesh. For the analysis of MMC with the FEA, many researchers have suggested the use of a unit cell concept instead of carrying out a complete FEA of each specimen to be studied, because the cost of computation the latter would be excessive (Balasivanandha Prabu et al., 2004). The use of the unit cell to find convergence in complex problems posed by the FEA is usually justified when the problem presents geometric symmetry, as well as periodicity, in its boundary conditions according to Sun and Vaidya (1996). This approach has the potential to provide an accurate approximation of the behavior of global mechanical properties, as well as serving as an indicator of residual stresses in the wires and matrix. In the current work, the unit cells that were considered for the FE study were those that were formed by sixteen complete wire openings, in which six complete wires are included (3 in the X and 3 in the Y direction). Also, half woven wires were located at the edges of each of the unit cells. The thickness of each cell was 8 mm (the same thickness as for the tensile and charpy tests). The proposed unit cell was considered for all configurations that were studied. It consisted of tetrahedral elements with linear formulation that represented a single circular stainless steel woven wire enclosed by a rectangular block of matrix recycled aluminum alloy. Fig. 4 depicts an example of the unit cell considered for the 1.41 mm × 0.32 mm configuration.

For each of the proposed unit cells, it was assured that quality tests, such as Jacobian, warpage and aspect ratio, fell within permitted bounds. The H-Method was chosen in this case to conduct a mesh sensitivity analysis and, thus, to enable the optimization of the size of each proposed unit cell Finite Element (FE) model. As a general rule, a finer mesh yields a more accurate answer in FEA. However, as the mesh becomes finer, so does the computing time. H-method entails analyzing a FE model with a coarse mesh and comparing the findings to those obtained by analyzing the same FE model with a finer mesh. This approach involves increasing the number of elements, nodes and, therefore, the degrees of freedom to solve. This procedure is repeated until the difference between the residual stresses obtained from two consecutive mesh sizes falls below a set threshold (in this case, 3%). Table 1 summarizes, for each of the unit cells FE models configurations that were studied, the number of elements, nodes as well as the average element size of the stainless steel AISI 304 woven wire mesh and of the aluminum matrix. As the table shows, the number of elements for all of the unit cell FE models greatly exceeds three million. Because all FE simulations were conducted as elastoplastic thermomechanical FEA, a considerable computational cost was probably involved due to the non-linearity of the problem. All FEA were simulated by an Intel Xeon Silver processor computer with a CPU of 2.1 GHz (32 processors) and 128 GB of random access memory (RAM).

2.3.1. Material properties

As described in detail by Kroupa and Bartsch (1998), one way to determine the thermal residual stresses in MMC with a elastoplastic thermomechanical FEA begins by assuming that the wires and matrix are stress-free at the at the melting temperature of the matrix (T_m), and that the residual internal stresses reach their maximum value at room temperature (T_R). Determining the thermal residual stresses that arise within the unit cell in the solidification of an MMC by the FEM is reasonably easy if the temperature-dependent mechanical and thermal properties of both the matrix and wires are well known. These properties are usually determined by the elastoplastic stress-strain curves, Young's and Poisson's modulus, coefficients of thermal expansion, thermal conductivity and specific heat. In the current paper, the FEA proposed in

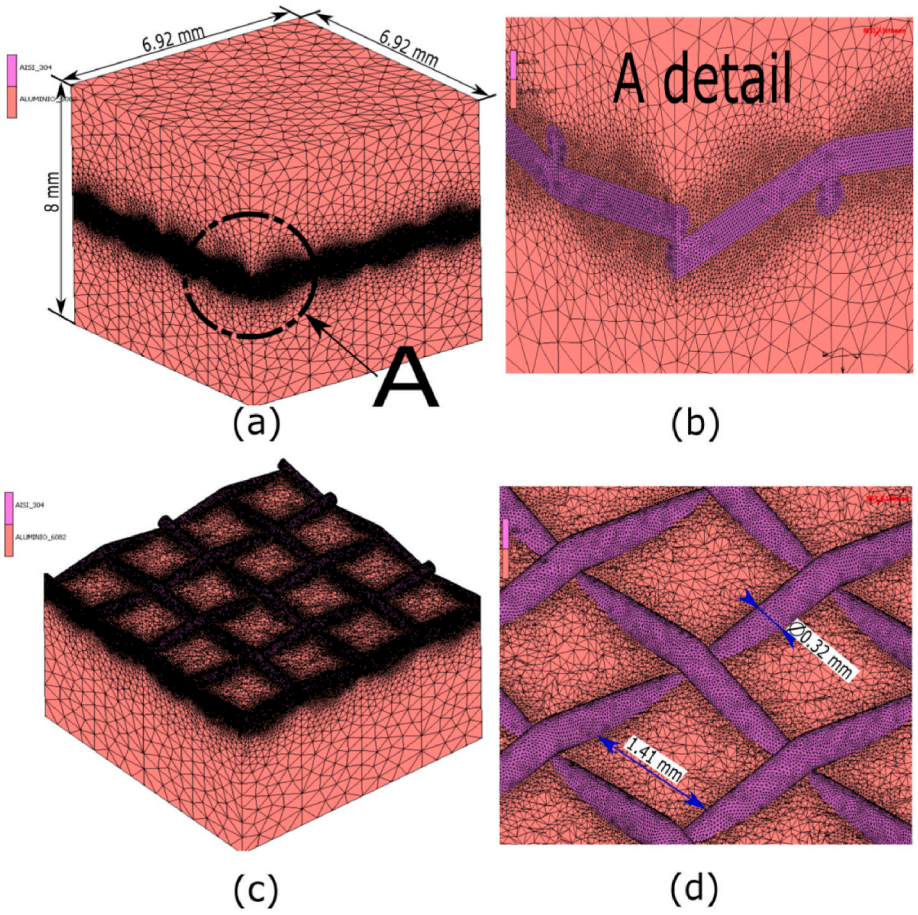

Fig. 4. Unit cell FE model proposed for the 1.41 mm × 0.32 mm configuration: (a) Complete unit cell showing its general dimensions. (b) Details of the corner of the unit cell in which the stainless steel wires can be seen. (c) Sectioned unit cell showing the stainless steel woven wire that has been considered for unit cells in this study. (d) Details of the stainless steel woven wire inserted into the middle of the unit cell.

Table 1
Number of elements and nodes of each configuration.

Configuration	N° Elements	N° nodes	Aver. Steel Wire Element Size	Aver. Aluminum Matrix Element Size
1.41 mm × 0.32mm	3164720	540835	0.031 mm.	0.43 mm.
1.81 mm × 0.5mm	6756517	1135871	0.032 mm.	0.45 mm.
2.177 mm × 0.6mm	7220628	1211785	0.041 mm.	0.46 mm.
2.72 mm × 0.75mm	5865900	984590	0.065 mm.	0.45 mm.
2.828 mm × 0.8 mm	4867420	817909	0.077 mm.	0.44 mm.

Table 2
Elastoplastic thermomechanical properties of recycled aluminum alloy EN AW 6082 and stainless steel AISI 304 woven wire mesh.

Properties	Recycled aluminum alloy		AISI 304	
	20 °C	660 °C	20 °C	660 °C
Young's modulus [MPa]	70000	41400	196000	150000
Poisson's ratio	0.33	0.33	0.3	0.3
Yield stregth [MPa]	280	10.5	473.2	309.5
Coef. thermal expansion [(mm/mm)/°C]	2.31e-05	3.19846e-05	1.61e-05	2.07e-05
Thermal conductivity [N/s.K]	215	196	13.3	22.4
Specific heat [mm^2/s^2.°C]	8.85e+08	1.113e+09	4.72e+08	6.04e+08

all MMC configurations assumed 660 °C and 20 °C for melting (T_m) and room temperature (T_R) respectively. The aforementioned variable-temperature mechanical and thermal properties were also assumed for the aluminum matrix and the stainless steel woven wires mesh. Because both materials have remarkably ductile behavior during the yielding process, the Von Mises yield criterion was considered in this case to describe the isotropic elastoplastic behavior of all MMC configurations. The values of the relevant elastoplastic thermomechanical properties of the recycled aluminum alloy EN AW 6082 matrix and stainless steel AISI 304 woven wire mesh at T_m and T_R appear in Table 2.

2.3.2. Boundary conditions

As previously mentioned, the aluminum blocks, from which each of the studied MMC configurations were manufactured by machining were cooled at a controlled temperature within the muffle furnace. The temperature declined from 800 °C inside the furnace from to a room temperature of 20 °C in a period of 20 h. As this controlled cooling occurred so slowly within the furnace, it was assumed that each of the zones of the recycled aluminum alloy EN AW 6082 block of stainless steel AISI 304 woven wire mesh and the stainless steel AISI 310S crucible shared the same temperature while cooling. This assumption that all materials that were contained within the muffle furnace shared the same temperature while cooling simplified the boundary conditions of the proposed elastoplastic thermomechanical FEA. Therefore, each of the nodes of each of the unit cell configuration was subjected to the same duration at the same incremental reduction in controlled temperature. In addition to this boundary condition, those surfaces of each unit cell

configuration, in which planes of symmetry have been assumed, have been considered. Also considered were other surfaces, such as the exterior one, that are allowed to deform (Ahmad et al., 2020). A consideration in the beginning of the FEA was that the initial temperature of all the nodes of the unit cell was 660 °C. Another assumption was that, and at the end of the simulation (18 h later), after the cooling curve had been fully applied, the temperature of each of these nodes would be room temperature (20 °C).

2.4. Life Cycle Assessment (LCA)

Environmental and sustainability implications of goods, processes and material removal rates may be evaluated easily by the use of LCA. This is a user-friendly tool that was developed for that purpose. LCA is comprised of four phases. They are: (1) Firstly, the goals and scope of the study must be determined in order to build the basis for the research. (2) Then, the life cycle inventory must be completed. It collects all relevant data within the system (material and energy). (3) Next, the environmental impact assessment is carried out. It involves reviewing the findings of the indicators of all the impact categories that have been studied are detailed. (4) Finally, the interpretation of the results that have been subjected to a critical review, along with their supporting data. The assessment is conducted in compliance with ISO 14040/1404 (2006). The CML-IA Baseline V3.06/EU25 midpoint approach impact methodology and the Ecoinvent 3 environmental inventory database, which are implemented in Simapro® v.9.2.0.2. software, were used to implement the LCA in current work. The Ecoinvent database collects all data that was necessary to carry out the environmental inventory. This includes all activities and processes. The CML-IA Baseline was developed by the University of Leiden in the Netherlands (Guinée and Lindeijer, 2002). It is used extensively throughout Europe. Midpoints are regarded as connections in the cause-effect chain (environmental mechanism) in an impact category (Bare, 2000). The CMA-IA baseline considers these categories to be the following: Abiotic depletion fossil fuels (AD(fosil)), Abiotic depletion (Ab_Dep), Ozone Layer Depletion (Oz_La_Dep), Global warming (Glo_War), Fresh Water Aquatic Ecotoxicity (Fr_Wa_Ab_Ec), Human Toxicity (Hu_To), Terrestrial ecotoxicity (Te_Ec), Marine aquatic ecotoxicity (Ma_Aq_Ec), Eutrophication (Eu), Photochemical oxidation (Ph_Ox) and Acidification (Ac). In this case, the LCA focused on (1) obtaining the environmental impact of the MMC manufacturing process by casting and (2) subsequent machining of the tensile and charpy tests specimens for all stainless steel wire-strengthened configurations that were studied. The environmental impact was compared to that corresponding to specimens of recycled aluminum EN AW 6082 without reinforcement. The functional unit that was considered in this study was the one that corresponded to the mass of each of the specimens that had been manufactured for tensile and charpy tests. Gate-to-gate research was conducted. The system boundary was restricted to covering only the MMC manufacturing process in the laboratory. This ensured that the study was relevant to its intended purpose. Because this research is described as "gate-to-gate," the inputs utilized to compile the environmental inventory were supplied by the Ecoinvent 3 database, after considering each of the MMC's resources, energy consumption or emissions to the environment that appear in Table 3.

Table 3
Information necessary to construct the environmental inventory.

Energy/Material	Item description in Simapro® v.9.2.0.2. software
•Electric energy consumed by the muffle furnace [kJ].	•Electricity, (Europe without Swizerland) low voltage
•Electric energy consumed by machining [kJ].	•Electricity, (Europe without Swizerland) low voltage
•Stainless steel AISI 304 needed for manufacturing the specimens[kg].	•Stainless steel AISI 304 needed, {GLO} market for APOS, S
•Recycled aluminum EN AW 6082 6082 needed for manufacturing the specimens [kg].	•Aluminum scrap, Recycled Content cut-off | Cut-off, S), post-consumer {GLO} aluminum scrap, post-consumer,
•Aluminum shavings generated during machining that are melted again to manufacture the specimens [kg].	•Aluminum scrap, post-consumer (waste treatment) {GLO} market for aluminum scrap, post-consumer APOS, S Scrap steel {Europe without Switzerland} market for scrap steel APOS, S
•Stainless steel AISI 304 shavings that are no longer melted down to make new mmc and they are treated as waste [kg].	•Scrap steel {Europe without Switzerland}market for scrap steel APOS, S
•Flux/slag cleaner unsed in melting [kg].	•Flux, for wave soldering {GLO} market for APOS,
•Cutting and coolant fluids use in machining [kg].	•Lubricating oil {RER} market for lubricating oil Cut-off, S.

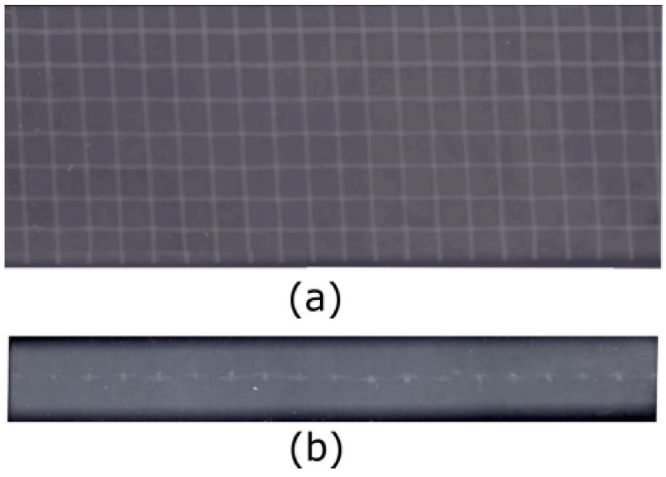

Fig. 5. Details of the radiogram of the toughness test specimen with a 2.828 mm × 0.8 mm configuration. (a) Top view. (b) Lateral view.

3. Results and discussion

3.1. Experimental results: tensile and toughnes

Probable faults and imperfections in the MMCs were analyzed using X-ray radiographic analysis in accordance with ISO 17636 (2013) after the specimens for the tensile and charpy tests were machined. In this case, radiograms (frontal an lateral) were taken for each of the specimens of the corresponding standardized tests. Fig. 5a shows a frontal radiogram whereas Fig. 5b shows a lateral radiogram. The radiographic evaluations showed the full incorporation of the steel grid into the aluminum matrix, free of flaws or imperfections that would have affected the mechanical properties of the specimens.

After it was confirmed that the specimens were already free of defects and imperfections, the yield and tensile strength values were determined using a Servosis universal testing machine type MAH-3000 (Servosis, Spain), whereas a Techlab Systems charpy impact testing machine type PIC-300/D (Techlab Systems, Spain) was used for the toughness test. Tensile and charpy tests results for all configurations that were studied (opening and wire diameters) and also for the recycled aluminum EN AW 6082 without reinforcement that appears in Table 4. In addition, this table shows the increment (%) achieved in yield, tensile strength and toughness with respect to the unreinforced aluminum matrix as well as the fiber volume ratio (VFR). The results indicate that the configuration of 2.177 mm × 0.6 mm (VFR = 1.27%) produced the highest yield, tensile strength and toughness (77.91 MPa, 81.11 MPa and 44 J respectively), despite being a configuration without the greatest wire diameter and VFR. The increment (%) achieved in this configuration for the yield, tensile strength and toughness with of the

Table 4
Values of yield stress, tensile strength and toughness obtained from the configurations studied.

Configuration	VFR	Yield stress	Yield stress	Tensile strength	Tensile strength	Toughness	Toughness
	[%]	*[MPa]*	*Incr. [%]*	*[MPa]*	*Incr. [%]*	*[J]*	*Incr. [%]*
1.41 mm × 0.32 mm	*0.58*	*12.83*	*−43.10*	*57.41*	*−19.58*	*20*	*25.00*
1.81 mm × 0.5 mm	*1.06*	*51.15*	*126.83*	*73.53*	*3.00*	*34*	*112.50*
2.177 mm × 0.6 mm	*1.27*	*77.91*	*245.50*	*81.11*	*13.62*	*44*	*175.00*
2.72 mm × 0.75 mm	*1.59*	*51.63*	*128.96*	*72.39*	*1.40*	*28*	*75.00*
2.828 mm × 0.8 mm	*1.73*	*53.04*	*135.21*	*74.71*	*4.65*	*20*	*25.00*
Unr. aluminum	–	22.55	–	*71.39*	–	*16*	-

unreinforced aluminum matrix were, 245.50%, 13.62% and 175.00%, respectively. In contrast, the lowest yield and tensile strength, which were even lower than the values for the unreinforced aluminum matrix (22.55 MPa, 71.39 MPa and 16 J), were found in the 1.41 mm × 0.32 mm configuration (VFR = 0.58%), measuring 12.83 MPa, 57.41 MPa and 20J respectively. The corresponding increment (%) achieved −43.10%, −19.58% and 25.00%. This implies that incorporating stainless steel AISI 304 into an aluminum matrix is not ideal for setups with openings and wire reduced diameters, because this may lessen the wettability of the interaction between the aluminum matrix and the stainless steel. However, it is not possible for large opening and wire diameter to improve yield, tensile strength and toughness, as the 2.828 mm × 0.8 mm configuration (VFR = 1.73%) does not have the best mechanical properties. In this configuration, the increment (%) achieved for the yield, tensile strength and toughness were 135.21%, 4.65% and 25.00% respectively. These results were compared with those of other configurations and casting processes studied several decades ago for metal matrix aluminum alloy that is reinforced with stainless steel fibers. No further recent references have been found in which these mechanical properties have been investigated for aluminum alloy-stainless steel fibers MMC. Thus, for example, during the 1970s (Pinnel and Lawley., 1970) studied the behavior of aluminum-stainless steel continuous fiber that was produced by vacuum hot-pressed for determination of yield strength. The results for the tensile test showed a yield strength increment of 685% when the VFR was 33%. The increment was 185% when VFR was 5%. Others authors, such as Pattnaik and Lawley (1974) conducted research on aluminum alloy-stainless steel fibers produced by squeeze casting to determine the tensile strength under different cooling curves. The results show a tensile strength increment of 2120% when the VFR was 19%. The increment was 715% when the VFR was 6.5%. A few years later, Bhagat (1988) studied the aluminum-stainless steel wires produced by high pressure squeeze casting. The results showed that, when VFR assumed values of 0.2% and 0.4%, the tensile strength increments obtained were 88.90% and 211%, respectively. These results showed that the increment (%) for the yield strength achieved in the current work for the configuration of 2.177 mm × 0.6 mm (VFR = 1.27%) is even greater than the values obtained by Pinnel and Lawley (1970) with VFR = 5% despite the greater technical complexity of the vacuum hot-pressed process than gravity casting and requires more energy. In contrast, the increment (%) of the tensile strength achieved in the configuration of 2.177 mm × 0.6 mm are much lower if any value of VFR obtained by the cited references (Pinnel and Lawley., 1970; Pattnaik and Lawley, 1974; Bhagat, 1988). This suggests that the novel MMC that is described in this study has a very large yield strength, while the tensile strength has somewhat lower values. This lead us to assume that the plastic deformations that this material is capable of withstanding are less. Moreover, Table 4 indicates that, as the wires diameter and VFR increase, the toughness also increases. This relationship is maintained until wire diameter and VFR are 0.6 mm and 1.27%, respectively, being the value of toughness the highest obtained (44 J). For larger values of diameter and VFR of 0.6 mm and 1.27%, it is the opposite, that is, as the wires diameter and VFR increase, the toughness decreases. It is when the wire diameter and VFR are 0.8 and 1.73%, respectively, when the minimum toughness value (20 J) is obtained again. These last results are also in agreement with those obtained by other authors. However no references have been found in which toughness has been investigated in aluminum-stainless steel fibers MMC. For example, Alaneme and Bodunrin (2013) studied the mechanical behavior of aluminum alloy 6063 reinforced with Al_2O_{3p} MMC. The values obtained for toughness showed that, as VFR increased, the toughness values declined. The range of values that was studied was VFR = 6% to VFR = 18%. Other authors such as Dwivedi et al. (2019) studied the toughness in an MMC that was based on an AA 6061 alloy reinforced with Al_2O_3 with different VFR values. The results showed that, as the VFR values increased, the toughness values decreased, as occurs in the current paper from VFR = 1.27%. Finally, it can be concluded that, the values obtained for any of the configurations that are proposed in the current research work reflect a significant increase in the mechanical property provided by the unreinforced aluminum matrix. These results are in agreement with those obtained by other researchers. This suggests that the MMC that this paper proposes has a significant ability to withstand dynamic and impact loads.

3.2. Environmental impact analysis

Tables 5 and 6 show the environmental impact of manufacturing the MMC specimens that underwent the tensile and charpy tests for all proposed configurations. These tests were conducted in accordance with Simapro® v.9.2.0.2. software considering the CML-IA baseline V3.06/EU25 methodology. These tables show that some environmental impacts produced very low values in their categories (Abiotic depletion (Ab_Dep), Ozone Layer Depletion (Oz_La_Dep) and Photochemical oxidation (Ph_Ox), whereas the remaining impacts are quite significant. The main reason for this is that the categories that generates the greatest environmental impact are those that are related to raw material consumption, energy and waste generated by the MMC manufacturing process (Corral et al., 2022). The production of MMC's requires the contribution of different materials (reinforcement and matrix), as well as the casting of the latter, which requires significant energy consumption. Although there are quite a few LCA reports on casting processes, there are hardly any references to MMC's production. For example, Santiago-Herrera et al. (2022) analyzed the production of a metal matrix based on aluminum alloy reinforced with TiO_2 nanoparticles by using both, green sand and low pressure die casting, using the ILCD 2011 Midpoint methodology. The lowest environmental impacts obtained for both processes were, as obtained in the current work, the Photochemical oxidation (Ph_Ox), Ozone Layer Depletion (Oz_La_Dep) and Human Toxicity (Hu_To). The greatest environmental impact that is observed in both tables is the one that corresponds with Marine Aquatic Ecotoxicity (Ma_Aq_Ec). The value obtained is high, but it is within the values considered as reasonable when these processes are considered. This environmental impact is generated for the most part by electricity generation processes (Atilgan and Azapagic., 2016; McNamara et al., 2016), in processes where materials have been recycled or treated, and certain heavy metals have been emitted (de Koning and Korenromp., 2004), or in machining processes (Aslan et al., 2019) as it happens in the current paper. Thus, to produce a specimen for the charpy test with the 1.41 × 0.32 mm configuration, 30% of this impact is provided by the

Table 5
Environmental impact values that are associated with the production of MMC specimens for the tensile tests.

Environmental Impact	*Configurations [mm x mm]*					
	*1.41 × 0.*32 mm	1.81 × 0.5 mm	2.177 × 0.6 mm	2.72 × 0.75 mm	2.828 × 0.8 mm	Unr. Alum.
Ab_Dep [kg Sb eq.]	9.9075E-4	9.9152E-4	9.9185E-4	9.9234E-4	9.9257E-4	9.8986E-4
Ab_Dep (fosil) [MJ]	484.5448	484.7854	484.8908	485.0495	485.1197	484.2544
Glo_War [kg CO2 eq.]	17.5141	17.5388	17.5496	17.5659	17.5731	17.48436
Oz_La_Dep [kg CFC-11 eq.]	5.1418E-6	5.1429E-6	5.1434E-6	5.1441E-6	5.1444E-6	5.1404E-6
Hu_To [kg 1.4-DB eq.]	18.9906	19.4269	19.6183	19.9068	20.0339	18.4626
Fr_Wa_Ab_Ec [kg 1.4-DB eq.]	142.8984	142.8994	142.8985	142.8938	142.8956	142.9067
Ma_Aq_Ec [kg 1.4-DBeq.]	57354.503	57426.39	57457.616	57503.901	57525.192	57269.714
Te_Ec [kg 1.4-DBeq.]	0.0990	0.0996	0.0998	0.1001	0.1003	0.0984
Ph_Ox [kg C_2H_4 eq.]	4.5864E-3	4.5944E-3	4.5979E-3	4.6032E-3	4.6055E-3	4.5767E-3
Ac [kg SO_2 eq.]	0.1015	0.1016	0.1016	0.1017	0.1018	0.1013
Eu [kg PO_4 eq.]	0.04787	0.04791	0.04793	0.04795	0.04797	0.04782

Table 6
Environmental impact values that are associated with the production of MMC specimens for the proposed toughness tests.

Environmental Impacts	Configurations [mm x mm]					
	1.41 × 0.32 mm	1.81 × 0.5 mm	2.177 × 0.6 mm	2.72 × 0.75 mm	2.828 × 0.8 mm	Unr.alum.
Ab_Dep [kg Sb eq.]	1.0268E-3	1.02747E-3	1.0276E-3	1.0284E-3	1.0283E-3	1.0260E-3
Ab_Dep (fosil) [MJ]	499.2726	499.5082	499.6120	499.9271	499.8705	498.9867
Glo_War [kg CO2 eq.]	17.8628	17.8869	17.8975	17.9191	17.9219	17.8335
Oz_La_Dep [kg CFC-11 eq.]	5.2965E-6	5.2976E-6	5.2980E-6	5.3004E-6	5.2995811E-6	5.2952E-6
Hu_To [kg 1.4-DB eq.]	19.4202	19.8555	20.0464	20.3408	20.4624	18.8932
Fr_Wa_Ab_Ec [kg 1.4-DB eq.]	148.4341	148.37565	148.3526	148.3653	148.3190	148.4988
Ma_Aq_Ec [kg 1.4-DBeq.]	58969.941	59027.948	59054.008	59112.154	59116.343	58898.296
Te_Ec [kg 1.4-DBeq.]	0.1001	0.1006	0.1008	0.1012	0.1013	0.0995
Ph_Ox [kg C_2H_4 eq.]	4.6974E-3	4.7052E-3	4.7086E-3	4.7153E-3	4.7165E-3	4.6879E-3
Ac [kg SO_2 eq.]	0.1037	0.1039	0.1039	0.1040	0.1041	0.1036
Eu [kg PO_4 eq.]	0.04857	0.04861	0.04863	0.04867	0.04867	0.04852

consumption of electricity for melting and machining the specimens, 52% is provided by the use of recycled aluminum and 17% is provided by the lubricant used in the machining process. Another significant environmental impact is one that corresponds to Abiotic Depletion Fossil Fuels (AD(fossil)). For example, to produce the same specimen for the charpy test, the 78% of this environmental impact is provided by the cutting fluids and coolants that re necessary to machine the specimens, whereas 19% is provided the consumption of electricity for melting and machining the specimens. Cutting fluids and coolants are often composed of oil, chemicals products and a substantial quantity of water. They have a significant environmental effect. Thus, it is not surprising that cutting fluids are the generators of the Abiotic Depletion Fossil Fuels (AD(fossil)) impact (Li (2015)). Similarly, the tables also indicate that all environmental impacts yield higher values for the manufacture of the toughness test than for the tensile test specimens. For example, the Global warming (Glo_War) values obtained for the manufacture of the tensile test MMC specimens in the 2.828 mm × 0.8 mm configuration are 17.573164 kg CO2 eq. but is 17.921961 kg CO2 eq. for the toughness test. The primary reason for this is that the manufacturing of specimens for the toughness test always requires a greater amount of material to be machined and, therefore, greater energy consumption and waste generation than the in manufacturing specimens for the tensile test. It should be noted that the manufacture of toughness and test specimens always begins with an recycled aluminum alloy EN AW 6082 block of dimensions 190 mm × 70 mm x 50 mm that has been cast and into which the stainless steel AISI 304 woven wires have been inserted. Also, as the diameter of the stainless steel AISI 304 woven wires increases, the environmental impact also increases. According to both tables, the greatest environmental impact is associated with the configurations that have the greatest wire diameters and greatest wire opening. For example, for the manufacturing of the tensile tests MMC specimens (Table 5), the corresponding values for Acidification (Ac) for the 1.41 mm × 0.32 mm and 2.828 mm × 0.8 mm configurations are 0.1015108 kg. SO2 eq. and 0.10182439 kg. SO2 eq. respectively. This is due mainly to the fact that, as the stainless steel AISI 304 woven wires diameter increases, the amount of steel in each of the specimens for both tests also increases. Therefore, the consumption of raw materials increases. The tables also indicate that the manufacture of the recycled aluminum EN AW 6082 without reinforcement specimens for both tests are those that generate the least impact. This was expected, as they do not contain stainless steel AISI 304 woven wires. Thus, as Table 5 shows, the greatest increase in environmental impact (in %) of recycled aluminum EN AW 6082 without reinforcement for the manufacture of a specimen for the tensile test according to the 2.828 mm × 0.8 mm configuration corresponds to the Human Toxicity (Hu_To) impact (8.51%). However, it can also be determined from Table 6 that, for the manufacture of a specimen for the toughness tests with this same 2.828 mm × 0.8 mm configuration, the greatest increase also corresponds to Human Toxicity (Hu_To) with the latter having a value of 8.30%. Similar result were obtained by Yusuf et al. (2021). In their work, the authors performed an LCA using the ReCiPe methodology for two different materials: recycled aluminium alloy (AA6061) and a composite of aluminum (AA6061) reinforced with 2% of particles of alumina. In this study, the greatest increase in environmental impact (in %) of recycled aluminum alloy (AA6061) was also associated with the Human Toxicity (Hu_To). The value obtained in this case was 12.8%. More recently, Eguía-Cambero et al. (2022) developed a LCA preliminary study of some configurations of AISI 304 stainless steel bidirectional continuous fibers inserted in recycled aluminum EN AW-6082. In this case, the environmental inventory considered the energy required for the melting and machining the tensile and charpy tests specimens. The Abiotic depletion (Ab_Dep), Global warming (Glo_War), Human Toxicity (Hu_To), and Acidification (Ac) environmental impacts were determined. In their study, the greatest increase in environmental impact (in %) of recycled aluminum alloy EN AW-6082 was the Acidification (Ac) environmental impact when the increment reached was 5.02%, which is much higher than the values obtained in the current paper, which were approximately 0.2%.

3.3. Finite Element Analysis: residual stresses

After all of the unit cell FE model configurations were simulated, with the thermal residual stresses in the local X direction of the unit cell (RS_X) and the thermal residual stresses in the local Y direction of the unit cell (RS_y) for the stainless steel woven wires, the aluminum matrix and the wire/matrix interfaces were obtained. Fig. 6a and b shows the RS_X that appears in the stainless steel woven wires for the 1.41 mm × 0.32 mm and 2.828 mm × 0.8 mm configurations, respectively. In similar fashion, Fig. 6c and d shows the RS_Y that appears in the stainless steel woven wires of the 1.41 mm × 0.32 mm and 2.828 mm × 0.8 mm configurations. In both figures, it can be seen that the RS_X and RS_Y are very similar for the same configuration ($RS_X = -18.45$ MPa vs $RS_Y = -19.25$ MPa, and $RS_X = -5.79$ MPa vs $RS_Y = -6.48$ MPa). This is due mainly to the symmetry of the proposed unit cells FE models. The figures also show that the configuration that has the smallest wire diameter (Ø0.32 mm and VFR = 0.58) has the highest values of compressive residual stress.

Also, Fig. 7a and b shows the RS_X that appears in the aluminum matrix and wire/matrix interfaces of the 1.41 mm × 0.32 mm and 2.828 mm × 0.8 mm configurations. Fig. 7c and d shows the RS_Y in the aluminum matrix and wire/matrix interfaces of the 1.41 mm × 0.32 mm and 2.828 mm × 0.8 mm configurations, respectively. As it happened with the residual stresses of the stainless steel woven wires shown in Fig. 6, the RS_X and RS_Y obtained for the matrix and wire/matrix interfaces are similar for the same configuration, as shown in Fig. 7. This figure also indicate that, for the wire/matrix interfaces, the configuration with the smallest wire diameter and VFR produces the highest values of compressive residual stress, as occurred with the stainless steel woven wires. The opposite happens with the matrix. That is, the configuration with the greatest wire diameter and VFR has the highest values of compressive residual stress.

Table 7 provides a summary, for all configurations studied, the RS_X and RS_Y that appear in the center of the unit cells FE models of the stainless steel woven wires, aluminum matrix and wire/matrix interfaces. The results show that, for the same configuration, the RS_X and RS_Y are very similar. This was expected due to the symmetry of the unit cells that FE models proposed. In addition, Table 7 shows how, as the diameter of the wire and the VFR declines, the RS_X and RS_Y increases for stainless steel woven wires and wire/matrix interfaces (compressive values). However, for the matrix, as the diameters of the wire and VFR increase, the RS_X and RS_Y also increase (compressive values). This last could be due to the larger the size of the reinforcing element and the greater the distortion it causes on the matrix. The thermal residual stresses determined in this study with the FEA are mainyorly in accordance with what was obtained by other researchers, despite the fact that the materials that they had proposed for both the fibers and the matrix differ greatly from those analyzed in this paper. In the recent past, there have been no in-deep studies of the thermomechanical elastoplastic behavior of stainless steel fibers or woven in aluminum matrix to determine the thermal residual stresses have involved the FEA. Thus, for example, Shoukry et al. (2007) studied the effects of VFR on the reinforcement/matrix interfaces of Alumina/Titanium (Al2O3/Ti–6Al-4Va) MMC. The results showed that, as the values of VFR increased from 10% to 30%, the compressive thermal residual stresses on the interface decreased. This same effect was observed in the current work, as shown in Table 7. Others authors, such as Ahmad et al. (2020), determined the thermal residual in RS_X for both, matrix and reinforcing material, in an a ceramic/metal SCS-6/Ti–6Al–4V composite. In this case, the reinforcing material was inserted into the matrix in a short fiber form. The thermal residual stresses on the reinforcement material were compressive residual stresses, whereas the stresses in the matrix were tensile residual stresses. The values obtained for the matrix (as tensile stresses) are not in agreement with the results of the current work, as they should be compressive values. Similarly, González-Lezcano et al. (2023) investigated for ceramic-reinforced metal matrix composites, the RS_X in the reinforced/matrix interfaces, reinforcing material and matrix. In their case, the reinforcing material was inserted into the matrix in particle form. The results showed RS_X with compressive values for both, reinforced/matrix interfaces and reinforcing material. They are in agreement with the values obtained from our current work. However, the RS_X for the matrix was as tensile stresses. This result does not agree with the

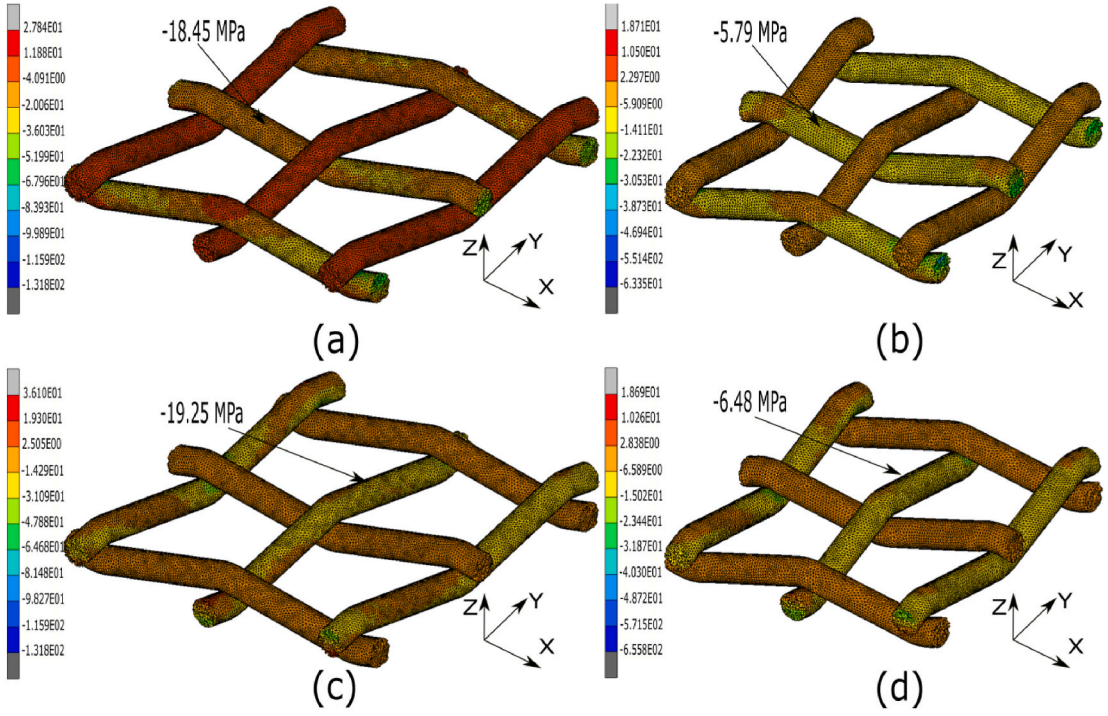

Fig. 6. Residual stresses of the stainless steel woven wires: (a) RS_X of the 1.41 mm × 0.32 mm configuration. (b) RS_X of the 2.828 mm × 0.8 mm configuration. (c)) RS_Y of the 1.41 mm × 0.32 mm configuration. (d) RS_Y of the 1.41 mm × 0.32 mm configuration.

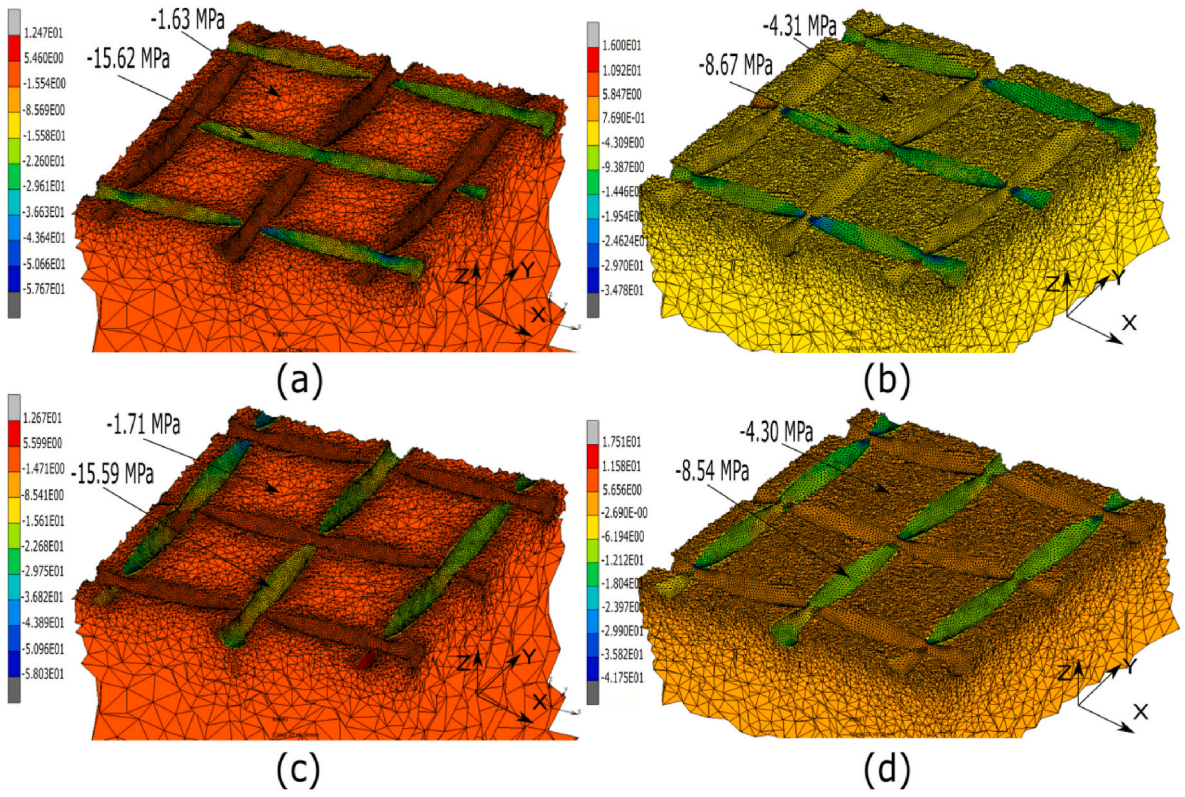

Fig. 7. Residual stresses for the for the aluminum matrix and for the wire/matrix interfaces: (a) RS_X of the 1.41 mm × 0.32 mm configuration. (b) RS_X of the 2.828 mm × 0.8 mm configuration. (c)) RS_Y of the 1.41 mm × 0.32 mm configuration. (d) RS_Y of the 2.828 mm × 0.8 mm configuration.

Table 7
Local X direction (RS_X) and local Y direction (RS_y) residual stresses for the stainless steel woven wires, aluminum matrix and wire/matrix interfaces that appear in the center of the unit cells FE models proposed.

Configuration	VFR	$RS_{x\ (wire)}$	$S_{y\ (wire)}$	$RS_{x\ (interface)}$	$RS_{y\ (interface)}$	$RS_{x\ (matrix)}$	$RS_{y\ (matrix)}$
	[%]	[MPa]	[MPa]	[MPa]	[MPa]	[MPa]	[MPa]
1.41 mm × 0.32 mm	*0.58*	*−18.45*	*−19.25*	*−15.62*	*−15.59*	*−1.63*	*−1.71*
1.81 mm × 0.5 mm	*1.06*	*−13.02*	*−13.84*	*−11.58*	*−11.52*	*−3.25*	*−3.28*
2.177 mm × 0.6 mm	*1.27*	*−10.48*	*−11.18*	*−9.98*	*−9.87*	*−3.89*	*−3.79*
2.72 mm × 0.75 mm	*1.59*	*−6.89*	*−7.56*	*−8.73*	*−8.65*	*−4.23*	*−4.21*
2.828 mm × 0.8 mm	*1.73*	*−5.79*	*−6.48*	*−8.67*	*−8.54*	*−4.31*	*−4.30*

result obtained in our work since the RS_X for the matrix was as compressive values. This difference in the stresses obtained for the matrix could be due to the size of the fibers or the particles that act as a reinforcing element. In Tables 7 and it can be seen that, as the diameter of the wire become smaller, the residual stresses on the matrix become less (compressive values). This suggests that, if the diameter of the wire was less than 0.32 mm, the residual stresses on the matrix could even reach positive values. However, the results in the current work are in agreement with what was stated by Aghdam and Morsali. (2014). Their contention was that to prevent the yielding of a MMC, the compressive thermal residual stresses in the reinforcing material, matrix, and matrix/reinforcement interfaces should be as minimal as feasible.

3.4. SEM-EDX analysis

To ensure that the wettability of the interaction between the aluminum matrix and the stainless steel is fully achieved, all wire configurations were analyzed after the standardized tests were completed. This was done by an 18 kV operating voltage on an HITACHI-S-2400 Scanning Electron Microscope (SEM). After this was completed, a qualitative examination was conducted using a Quantax 200 Energy Dispersive X-ray (EDX) spectroscope (Bruker, Germany) that was equipped with the ESPRIT 1.9 microanalysis software and an XFlash 5010/30 detector. Fig. 8 shows that the recycled aluminum EN AW 6082 alloy matrix was almost completely filled with stainless steel AISI 304 woven wire mesh for the 2.828 mm × 0.8 mm (Figs. 8a) and 1.41 mm × 0.32 mm (Fig. 8b) configurations. Hence, it exhibits excellent wetting chacteristics, which would guarantee good adherence of the aluminum to the stainless steel fibers (Güler et al., 2014).

In addition, this figure shows a narrow area with a much finer particle size around the stainless steel AISI 304 wires. This corresponds to the matrix-reinforcement interface. Table 8 lists the significant elements of this research, whereas Fig. 9 displays the EDX analysis zones for the 2.828 mm × 0.8 mm configuration on the EN AW 6082/AISI 304 microstructure. According to the results of the analysis, the interface consists of Fe, Al, Cr, Ni and Mn elements, whereas the matrix includes only Al. Fe, Cr, Ni and Mn interfaces occur mainly in the wires that make up stainless steel AISI 304 reinforcement. Because of the high Fe and Al concentrations, one can say that the interface includes a substantial fraction of Al–Fe intermetallic. The remaining elements that appear in the EDX analysis (C, O, S, Si and Mg) probably had been contained in that the recycled aluminum.

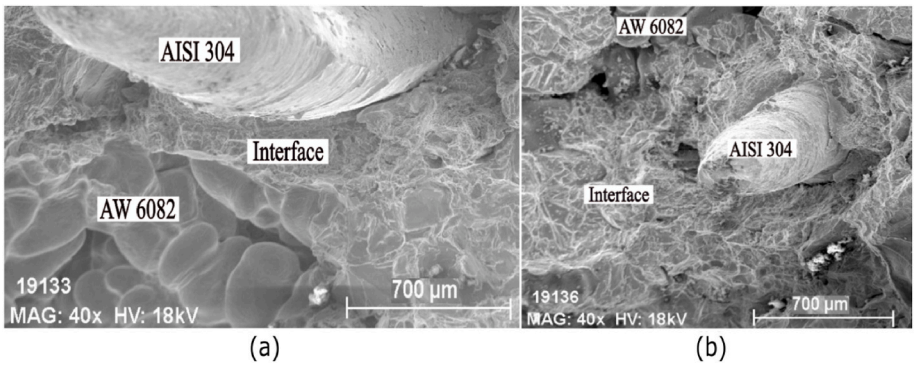

Fig. 8. SEM image of the recycled aluminum alloy EN AW 6082 matrix completely reinforced with stainless steel AISI 304 wires and the matrix-reinforcement interface at a magnification of 40X: (a) for the 2.828 mm × 0.8 mm configuration and (b) for the 1.41 mm × 0.32 mm configuration.

Table 8
Results of the EDS analysis in Fig. 9

Elements	Weigth(%)	Elements	Weigth(%)
Aluminium(Al)	51.77%	Carbon (C)	17.40%
Chromium(Cr)	2.91%	Oxigen (O)	11.46%
Iron (Fe)	8.55%	Sodium (S)	2.20%
Nickel (Ni)	1.06%	Manganese (Mn)	0.26%
Magnesium (Mg)	2.55%	Silicon (Si)	1.84%

4. Conclusions

This research involved an effort to explore the feasibility of producing a brand-new MMC as an alternative option for reducing aluminum waste generation and raw and energy consumption, and also for mitigating environmental effects. The most significant features of this MMC are: (1) the material matrix is recycled aluminum EN AW 6082, (2) the reinforcing material is stainless steel AISI 304 woven wire mesh that is intended for industrial and commercial use and (3) the brand-new MMC is manufactured by gravity casting.

The manufacturing process of the proposed MMC required the recycled aluminum to be melted in a muffle furnace, a flux/slag cleaner to be added to eliminate the waste and impurities, as well as for avoid oxidation of the molten aluminum, stainless steel woven wire mesh that is intended for industrial and commercial use to be inserted, and the specimens to be machined for standardized tensile and Charpy tests. An X-ray radiography analysis indicated that all specimens that were manufactured according to the described process did had no faults and imperfections. In addition, the wettability of the interaction stainless steel/aluminum and its elemental composition were determined by Scanning Electron Microscope (SEM) and Energy Dispersive X-Ray (EDX) respectively.

Five different opening and wire diameter configurations that were oriented at 0° of AISI 304 woven wire mesh that is intended for industrial and commercial use were studied. The yield, tensile strength and toughness of each of the new composite were determined, as well as their thermal residual stresses that arise during the production and environmental impact. A thermomechanical elastoplastic FEA that considers the cooling of the MMC has been proposed to determine the thermal residual stresses. Also, an LCA assessed the environmental impacts. The results were analyzed and discussed, and also compared to those produced with the recycled aluminum EN AW 6082 without reinforcement. Of all the configurations that have been studied, the best configuration of openings and wire diameters is the one that has the best mechanical properties and the least, thermal residual stresses and environmental impact arising during production.

The mechanical properties that have been obtained given an idea for various applications. This new lightweight MC that is manufactured by gravity casting could find use for example in the automotive and aerospace industries. Despite not having a larger wire diameter than other configurations that were examined, the configuration of 2.177 mm × 0.6 mm has achieved the maximum yield strength (77.91 MPa), tensile strength (81.11 MPa), and toughness (44 J). Nonetheless, the configuration of 1.41 mm × 0.32 mm has gave the lowest yield and tensile strength values (293 MPa and 1311 MPa). These last values are even lowers than those reported for aluminum without reinforcement (515 MPa and 1630 MPa). The same does not hold true for toughness (20 J). This indicates that inserting stainless steel AISI 304 into an aluminum matrix is not appropriate for applications with smaller openings and wire sizes, as the wettability of the interaction between the aluminum matrix and the stainless steel could decline.

The LCA indicates that the environmental impact obtained has been higher for the production of the toughness tests specimens and also when the diameter of the stainless steel AISI 304 woven wires has

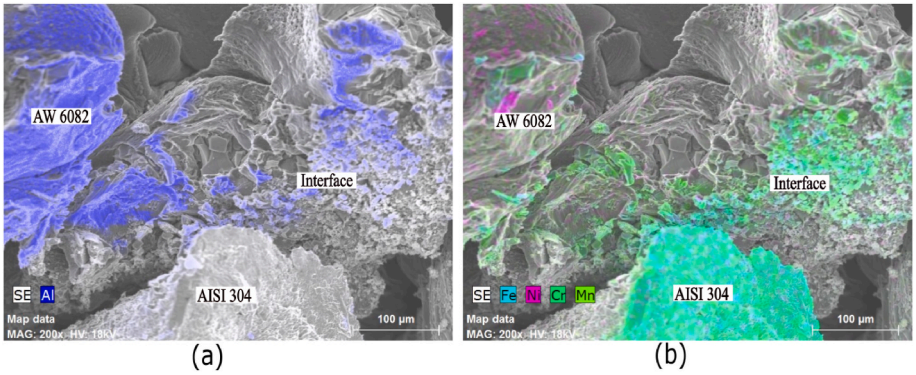

Fig. 9. EDX analysis: (a) traces of recycled aluminum alloy EN AW 6082 that appear in the matrix and in the interface and (b) traces of stainless steel AISI 304 appearing in the reinforcement and in the interface.

increased. This is due mainly because the manufacture of the toughness test specimens and configurations with a larger diameter of wire always requires a greater amount of material to be machined. This results in more energy and waste than in the manufacture of the tensile test specimens. It has also been observed that the greatest increase in environmental impact (in %) when it is compared recycled aluminum EN AW 6082 without reinforcement corresponds to the Human Toxicity (Hu_To) environmental impact. For example, for the 2.177 mm × 0.6 mm configuration, this increase has been 6.25% for the manufacture of the tensile test specimens, but 6.1% for the manufacture of the toughness tests specimens. This means that producing a laboratory specimen for tensile or toughness tests, and in extension to any mechanical component produced with the proposed MMC, would mean a relatively low increase in the environmental impact generated than if the specimens were produced with recycled aluminum EN AW 6082 without reinforcement.

The values obtained for the thermal residual stresses with the FEA have confirmed that, as the wire diameter and the fiber volume ratio (VFR) become smaller, the thermal residual stresses in the local X and Y directions (RS_X and RS_y) for both, wire/matrix interfaces and stainless steel woven wire mesh, are larger, whereas the opposite is true for the recycled aluminum matrix. That is, they become smaller. This suggests that, if the diameter of the wire was less than 0.32 mm, the residual stresses on the matrix could even reach positive values. In this work, all configurations studied have shown compressive values for the thermal residual stresses. Also, the values obtained for the 2.177 mm × 0.6 mm configuration have been as follows: for the wires ($RS_X = -10.48$ MPa and $RS_y = -11.18$ MPa), for the wire/matrix interfaces ($RS_X = -9.98$ MPa and $RS_y = -9.87$ MPa) and for the matriz ($RS_X = -3.89$ MPa and $RS_y = -3.79$ MPa). These results confirm the hypothesis that to prevent the yielding of a MMC, it is desirable that both, the reinforcing material and the wire/matrix interfaces, of any MMC have compressive thermal residual stresses as low as possible.

For future work, extending the current study that is focused on "gate-to-gate" to "cradle to gate" or even "cradle to grave" is proposed. This will make it possible to gain a better perspective of the raw materials used for the manufacture of the proposed MMC, as well as its final recycling process once its useful life has ended. Also, it would be interesting to propose the use of other environmental impact analysis methodologies with an endpoint approach, such as ReCiPe or IPCC. Thus, the environmental impacts obtained could be grouped into three large levels, such as human health, biodiversity and resource scarcity. Because the manufacturing process in this case has involved gravity casting, manufacturing the proposed MMC using other processes such as vacuum hot-pressed casting or squeeze casting could give rise to much higher mechanical properties, without underestimate those that have been obtained in the current work. Finally, examining how different orientations of stainless steel AISI 304 woven wire mesh (for example at 45°) influence the mechanical properties would lead to a more precise and complete mechanical knowledge of the MMC proposed for different mechanical applications.

CRediT authorship contribution statement

Rubén Lostado-Lorza: Experimental works, Formal analysis. **Marina Corral-Bobadilla:** Experimental works, Formal analysis. **Saúl Íñiguez-Macedo:** Data curation, Formal analysis. **Fátima Somovilla-Gómez:** Experimental works.

Declaration of competing interest

The authors declare that they have no known competing financial interests or personal relationships that could have appeared to influence the work reported in this paper.

Data availability

No data was used for the research described in the article.

Nomenclature

Ac	Acidification
Ab_Dep	Abiotic Depletion
AD(fosil)	Abiotic Depletion of fossil fuels
Ae	Radial depth of cut
Ap	Axial depth of cut
Eu	Eutrophication
EDX	Energy Dispersive X-ray
FEA	Finite Element Analysis
FE	Finite Element
Fr_Wa_Ab_Ec	Fresh Water Aquatic Ecotoxicity
Glo_War	Global Warming
Hu_To	Human Toxicity
K	Unit constant for machining
LCA	Life Cycle Assessment
Ma_Aq_Ec	Marine aquatic ecotoxicity
MMC	Metal Matrix Composite
MRR	Metal Removal Rate
Oz_La_Dep	Ozone Layer Depletion
Ph_Ox	Photochemical oxidation
RSx (interface)	Thermal residual stresses in Y direction for wire/matrix interfaces
RSx (matrix)	Thermal residual stresses in X direction for matrix
RSx (wire)	Thermal residual stresses in X direction for matrix for wires
RSy (interface)	Thermal residual stresses in Y direction for wire/matrix interfaces
RSy (matrix)	Thermal residual stresses in Y direction for matrix
RSy (wire)	Thermal residual stresses in Y direction for matrix for wires
SEM	Scanning Electron Microscope
Te_Ec	Terrestrial Ecotoxicity
Tm	Melting temperature of the matrix
TR	Room temperature
Val	Total volume of aluminum to machine
VFR	Fiber volume ratio
Vf	Cutting speed
w	Specific energy for machining
η	Performance of the milling machine

References

Aghdam, M.M., Morsali, S.R., 2014. 9 - understanding residual stresses in metal matrix composites. In: Shokrieh, M.M. (Ed.), Residual Stresses in Composite Materials. Woodhead Publishing, pp. 233–255. https://doi.org/10.1533/9780857098597.2.233.

Ahmad, J., Santhosh, U., Chandu, S., 2020. A nonlinear analysis interpretation of off-Axis test results in metal matrix composites. Journal of Composites Science 4, 127. https://doi.org/10.3390/jcs4030127.

Alaneme, K., Bodunrin, M., 2013. Mechanical behaviour of alumina reinforced AA (6063) metal matrix composites developed by two - step stir casting process. Acta Tech. Corviniensis - Bull. Eng. 3, 105–110.

Aslan, J.F., Weber, L.I., Iannacone, J., Junior, J.L., Saraiva, V.B., Oliveira, M.M., 2019. Toxicity of drilling fluids in aquatic organisms: a review. Ecotoxicology and Environmental Contamination 14, 35–47. https://doi.org/10.5132/eec.2019.01.04.

Atilgan, B., Azapagic, A., 2016. Assessing the environmental sustainability of electricity generation in Turkey on a life cycle basis. Energies 9, 31. https://doi.org/10.3390/en9010031.

Balasivanandha Prabu, S., Karunamoorthy, L., Kandasami, G.S., 2004. A finite element analysis study of micromechanical interfacial characteristics of metal matrix composites. Journal of Materials Processing Technology, Proceedings of the International Conference in Advances in Materials and Processing Technologies 992–997. https://doi.org/10.1016/j.jmatprotec.2004.04.157, 153–154.

Bare, J.C., 2000. Life cycle impact assessment workshop summary. Midpoints versusEndpoints: Int. I. LCA 5, 319–326.

Bhagat, R.B., 1988. High pressure squeeze casting of stainless steel wire reinforced aluminium matrix composites. Composites 19, 393–399. https://doi.org/10.1016/0010-4361(88)90127-9.

Board, U.C., 1988. Advanced Materials by Design. Office of Technology Assessment, Washington, DC.
Corral-Bobadilla, M., Lostado-Lorza, R., Somovilla-Gómez, F., Íñiguez-Macedo, S., 2022. Life cycle assessment multi-objective optimization for eco-efficient biodiesel production using waste cooking oil. J. Clean. Prod. 359, 132113 https://doi.org/10.1016/j.jclepro.2022.132113.
de Koning, R.H.-A., Korenromp, T.L.-R., 2004. Improvement of LCA Characterization Factors and LCA Practice for Metals. Institute of Environmental Sciences, Leiden University.
de Martini Fernandes, L., Lopes, J.C., Ribeiro, F.S.F., Gallo, R., Razuk, H.C., de Angelo Sanchez, L.E., de Aguiar, P.R., de Mello, H.J., Bianchi, E.C., 2019. Thermal model for surface grinding application. Int. J. Adv. Manuf. Technol. 104, 2783–2793. https://doi.org/10.1007/s00170-019-04101-6.
Diaz, N., Redelsheimer, E., Dornfeld, D., 2011. Energy consumption characterization and reduction strategies for milling machine tool use. In: Glocalized Solutions for Sustainability in Manufacturing, pp. 263–267.
Dwivedi, S., Srivastava, A., Maurya, N., Manish, M., 2019. Microstructure and mechanical properties of Al 6061/Al2O3/fly-ash composite fabricated through stir casting. Ann. Chimie Sci. Matériaux 43, 341–346. https://doi.org/10.18280/acsm.430510.
Eguía-Cambero, I.J., Lostado-Lorza, R., Corral-Bobadilla, M., Iñiguez-Macedo, S., Gómez, F.-S., 2022. Life Cycle Assessment (LCA) of recycled aluminum Metal Matrix Composites (MMC) reinforced with stainless steel bidirectional continuous fibers. In: 2022 7th International Conference on Smart and Sustainable Technologies (SpliTech). Presented at the 2022 7th International Conference on Smart and Sustainable Technologies (SpliTech), pp. 1–5. https://doi.org/10.23919/SpliTech55088.2022.9854271.
Fitzgerald, A., Proud, W., Kandemir, A., Murphy, R.J., Jesson, D.A., Trask, R.S., Hamerton, I., Longana, M.L., 2021. A life cycle engineering perspective on biocomposites as a solution for a sustainable recovery. Sustainability 13, 1160. https://doi.org/10.3390/su13031160.
González-Lezcano, R.A., del Río-Campos, J.M., Awad Parada, T., 2023. Influence of thermal residual stresses on the behaviour of metal matrix composite materials. Iran J Sci Technol Trans Mech Eng. https://doi.org/10.1007/s40997-023-00601-9.
Guinée, J.B., Lindeijer, E., 2002. Handbook on Life Cycle Assessment: Operational Guide to the ISO Standards. Springer Science & Business Media.
Güler, K., Kisasöz, A., Karaaslan, A., 2014. Investigation of Al/steel bimetal composite fabrication by vacuum assisted solid mould investment casting. Acta Phys. Pol. 126 https://doi.org/10.12693/aphyspola.126.1327.
International Aluminium Institute, 2009. Global aluminium recycling: a cornerstone of sustainable development. https://international-aluminium.org/wp-content/uploads/2021/09/Global-Aluminium-Recycling.pdf. (Accessed 26 September 2022).
Iqbal, A., Zhao, G., Suhaimi, H., Nauman, M.M., He, N., Zaini, J., Zhao, W., 2021. On coolant flow rate-cutting speed trade-off for sustainability in cryogenic milling of Ti–6Al–4V. Materials 14, 3429. https://doi.org/10.3390/ma14123429.
ISO 14044, 2006 [WWW Document]. ISO. URL. https://www.iso.org/cms/render/live/en/sites/isoorg/contents/data/standard/03/84/38498.html. January.19.22.
ISO, 2013. ISO 17636-1:2013 Non-destructive testing of welds — radiographic testing — Part 1: X- and gamma-ray techniques with film [WWW Document]. URL. https://www.iso.org/standard/52981.html. accessed 2.21.23.
ISO, 2015. ISO 14556:2015(en), Metallic materials — charpy V-notch pendulum impact test — instrumented test method [WWW Document]. URL. https://www.iso.org/obp/ui/#iso:std:iso:14556:ed-2:v1:en. accessed 2.21.23.
ISO, 2019. ISO 6892-1:2019 Metallic materials — tensile testing — Part 1: method of test at room temperature [WWW Document]. URL. https://www.iso.org/standard/78322.html. accessed 2.21.23.
Kroupa, J.L., Bartsch, M., 1998. Influence of viscoplasticity on the residual stress and strength of a titanium matrix composite after thermomechanical fatigue. Compos. B Eng. 29, 633–642. https://doi.org/10.1016/S1359-8368(98)00017-1.
Li, W., 2015. Efficiency of Manufacturing Processes. Springer.
McNamara, G., Fitzsimons, L., Horrigan, M., Phelan, T., Delaure, Y., Corcoran, B., Doherty, E., Clifford, E., 2016. Life cycle assessment of wastewater treatment plants in Ireland. Journal of Sustainable Development of Energy, Water and Environment Systems 4, 216–233. https://doi.org/10.13044/j.sdewes.2016.04.0018.
Mortensen, A., Llorca, J., 2010. Metal matrix composites. Annu. Rev. Mater. Res. 40, 243–270.
Mussatto, A., Ahad, I.U., Mousavian, R.T., Delaure, Y., Brabazon, D., 2021. Advanced production routes for metal matrix composites. Engineering Reports 3, e12330. https://doi.org/10.1002/eng2.12330.
Newswire, G., 2020. Metal Matrix Composite Market Size, Share & Trends Analysis Report by End-Use (Ground Transportation, Electronics), by Product (Refractory, Aluminum), by Region, and Segment Forecasts, pp. 2020–2027.
Öndin, O., Kıvak, T., Sarıkaya, M., Yıldırım, Ç.V., 2020. Investigation of the influence of MWCNTs mixed nanofluid on the machinability characteristics of PH 13-8 Mo stainless steel. Tribol. Int. 148, 106323 https://doi.org/10.1016/j.triboint.2020.106323.
Pattnaik, A., Lawley, A., 1974. Effect of elevated temperature exposure on the structure, stability, and mechanical behavior of aluminum-stainless steel composites. Metall. Trans. B 5, 111–122. https://doi.org/10.1007/BF02642934.
Pinnel, M.R., Lawley, A., 1970. Correlation of uniaxial yielding and substructure in aluminum-stainless steel composites. Metall. Mater. Trans. B 1, 1337–1348. https://doi.org/10.1007/BF02900252.
Requena, G., Garcés, G., Fernández, R., Schöbel, M., 2012. Determination of internal stresses in lightweight metal matrix composites. In: Neutron Diffraction. InTech, Rijeka, p. 257.
Santiago-Herrera, M., Ibáñez, J., Díez-Hernández, J., Tamayo-Ramos, J.A., Pabel, T., Kneissl, C., Alegre, J.M., Martel-Martín, S., Barros, R., 2022. Comparative life cycle assessment of green sand casting and low pressure die casting for the production of self-cleaning AlMg3-TiO2 metal matrix composite. Ecol. Indicat. 144, 109442 https://doi.org/10.1016/j.ecolind.2022.109442.
Sarikaya, M., Gupta, M.K., Tomaz, I., Danish, Mohd, Mia, M., Rubaiee, S., Jamil, M., Pimenov, D.Y., Khanna, N., 2021. Cooling techniques to improve the machinability and sustainability of light-weight alloys: a state-of-the-art review. J. Manuf. Process. 62, 179–201. https://doi.org/10.1016/j.jmapro.2020.12.013.
Sharma, A.K., Bhandari, R., Aherwar, A., Rimašauskienė, R., 2020. Matrix materials used in composites: a comprehensive study. Mater. Today: Proceedings, International Conference on Mechanical and Energy Technologies 21, 1559–1562. https://doi.org/10.1016/j.matpr.2019.11.086.
Sheng Li, D., Wisnom, M.R., 1994. Finite element micromechanical modelling of unidirectional fibre-reinforced metal-matrix composites. Compos. Sci. Technol. 51, 545–563. https://doi.org/10.1016/0266-3538(94)90088-4.
Shoukry, S.N., Prucz, J.C., Eluripati, R., Shankaranarayana, P.G., William, G.W., 2007. Multi-fiber unit cell for prediction of residual stresses in continuous fiber composites. Mech. Adv. Mater. Struct. 14, 531–540. https://doi.org/10.1080/15376490701585991.
Sun, C.T., Vaidya, R.S., 1996. Prediction of composite properties from a representative volume element. Compos. Sci. Technol. 56, 171–179. https://doi.org/10.1016/0266-3538(95)00141-7.
Umair, S., 2006. Environmental Impacts of Fiber Composite Materials : Study on Life Cycle Assessment of Materials Used for Ship Superstructure.
Walsh, R.A., 2001. Handbook of Machining and Metalworking Calculations. McGraw-Hill Education.
Wu, Y., Xia, C., Cai, L., Garcia, A.C., Shi, S.Q., 2018. Development of natural fiber-reinforced composite with comparable mechanical properties and reduced energy consumption and environmental impacts for replacing automotive glass-fiber sheet molding compound. J. Clean. Prod. 184, 92–100. https://doi.org/10.1016/j.jclepro.2018.02.257.
Yusuf, N.K., Lajis, M.A., Ahmad, A., 2021. Life cycle assessment on the direct recycling aluminium alloy AA6061 chips and metal matrix composite (MMC-AlR). International Journal of Integrated Engineering 13, 95–100.